Article published online: 2022-12-09

Novel Worm-like Micelles for Hydrochloride Doxorubicin Delivery: Preparation, Characterization, and *In Vitro* Evaluation

Ya-Ni Yang[1,#] Chen Ge[1,#] Jun He[1,*] Wei-Gen Lu[1,*]

[1] National Pharmaceutical Engineering Research Center, China State Institute of Pharmaceutical Industry, Shanghai, People's Republic of China

Pharmaceut Fronts 2022;4:e284–e294.

Address for correspondence Jun He, PhD, National Pharmaceutical Engineering Research Center, China State Institute of Pharmaceutical Industry, 285 Gebaini Road, Shanghai 201203, People's Republic of China (e-mail: chinaynhe@163.com).

Wei-Gen Lu, PhD, National Pharmaceutical Engineering Research Center, China State Institute of Pharmaceutical Industry, 285 Gebaini Road, Shanghai 201203, People's Republic of China (e-mail: sipiluwg@163.com).

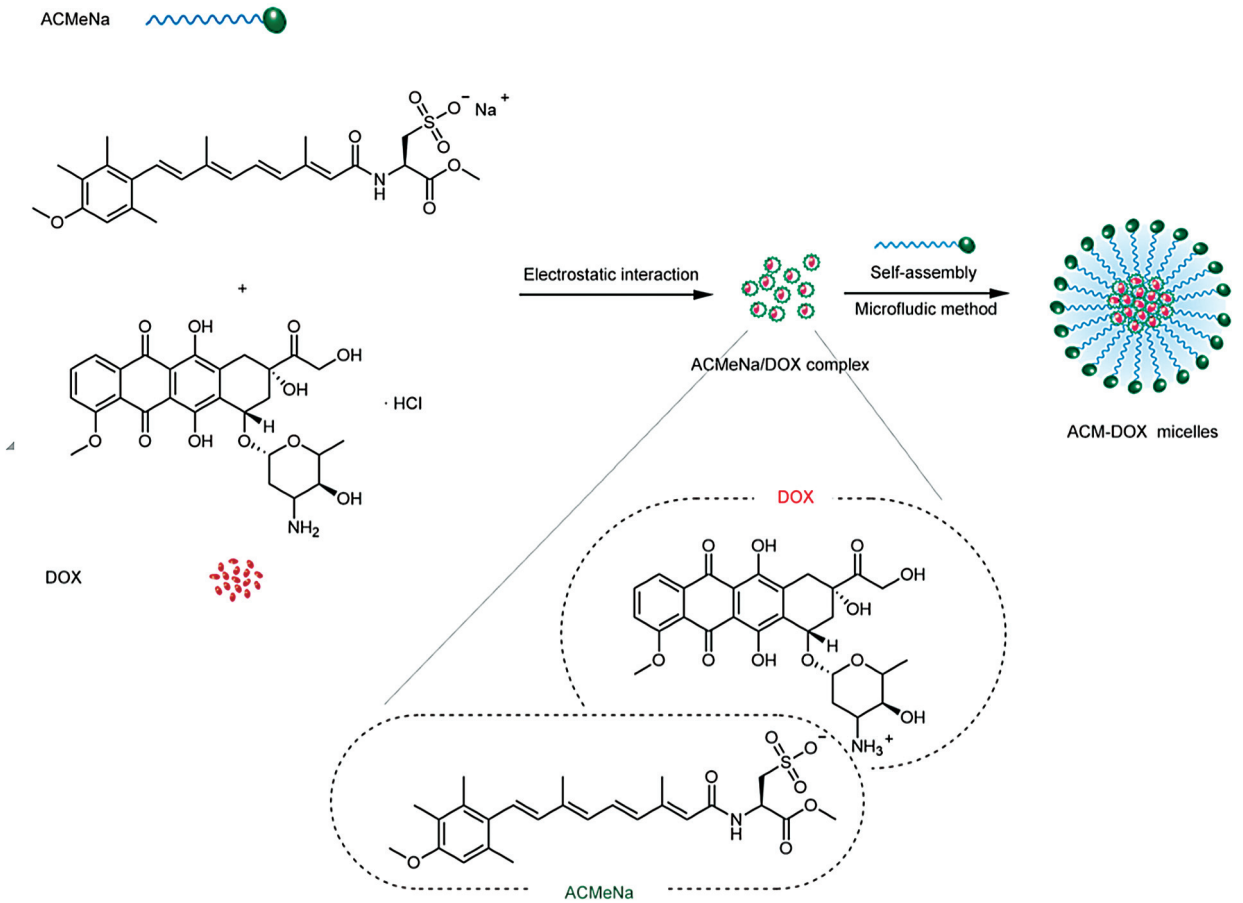

[#] *These authors contributed equally to this work.*

received
April 10, 2022
accepted
September 27, 2022

DOI https://doi.org/10.1055/s-0042-1758191.
ISSN 2628-5088.

Georg Thieme Verlag KG, Rüdigerstraße 14, 70469 Stuttgart, Germany

Abstract

Doxorubicin hydrochloride (DOX) is one of the widely used antineoplastic agents in treating various cancers, yet it is always associated with the occurrence of adverse reactions that limit its clinical use. Currently, encapsulating DOX in micelles may represent a promising strategy to reduce toxicity and side effects of the drug. This study aimed to explore a novel acitretin-based surfactant (ACMeNa) with good solid stability to encapsulate DOX to form micelles (ACM-DOX). In this work, ACM-DOX micelles were prepared by a microfluidic method free of organic solvents. The characteristics of ACM-DOX micelles were assessed, including morphology, particle size, stability, entrapment efficiency, and drug loading. An *in vitro* cytotoxicity experiment of the micelles on MDA-MB-231 (a human breast cancer cell line) was also performed. The micelle formation mechanism suggested that the insoluble ACMeNa/DOX complex was formed by electrostatic interaction, and subsequently encapsulated by self-assembly into micelles. The designed ACM-DOX micelles had an average particle size of 19.4 ± 0.2 nm and a zeta potential of -43.7 ± 2.4 mV, with entrapment efficiency and drug loading efficiency of $92.4 \pm 0.5\%$ and $33.4 \pm 0.3\%$, respectively. The ACM-DOX micelles had worm-like structures under a Cryo-transmission electron microscope and exhibited good stability within 8 hours after reconstitution and 4- to 32-fold dilution of its reconstituted solution. ACM-DOX micelles released 80% of DOX within 24 hours in a medium of $pH = 5.0$, and its drug profile can be described by a first-order model. Moreover, ACM-DOX micelles showed cytotoxicity against MDA-MB-231 in a dose-dependent manner, and displayed a higher antitumor activity as compared with free DOX, with IC_{50} values of DOX and ACM-DOX micelles being 6.80 ± 0.50 and 4.64 ± 0.32 μg/mL, respectively. Given above, ACMeNa has great application potential as a DOX carrier for the treatment of cancers.

Keywords

- doxorubicin hydrochloride
- ACMeNa surfactants
- micelles
- microfluidics

Introduction

Doxorubicin hydrochloride (DOX) is one of the widely used powerful antineoplastic agents in the clinical practice for the treatment of a wide range of cancers, including hematological malignancies, soft tissue sarcomas, and solid tumors.[1] It is generally used in its hydrochloride form to increase drug solubility in water. Unfortunately, when it was intravenously administered, due to its low binding rate to plasma proteins, rapid distribution occurs in the heart, kidney, liver, spleen, and lung, with bone marrow suppression and significant dose-dependent cardiotoxicity.[2,3] Severe adverse reactions, such as congestive heart failure, have limited its clinical application.[4] Taking these into account, encapsulating drugs into nanoparticles appears to have distinct advantages, including controlling drug delivery, improving drug pharmacokinetics, enhancing efficacy, and reducing side effects.[5] The developed drug delivery strategies provide an alternative to simple intravenous infusion of aqueous solution of DOX to reduce toxicity and side effects of the drug.[5,6] The most successful one is Doxil, an unique form of liposomal DOX, that was approved by Food and Drug Administration in 1995. Doxil is undoubtedly successful in reducing DOX cardiotoxicity,[7,8] but the process for liposome preparation is complex, leading to a great increase in the cost of drug manufacturing and bringing some side effects caused by lipid components.[9]

Micelles are self-assembled core–shell nanocarriers formed by surfactants or polymers. Micellar drug formulation, due to its smaller particle size (10–100 nm), could passively target solid tumors (even poorly permeable tumors) and internalize cells more effectively.[10] The formulation has high vascular permeability, which is not easy to be opsonized by plasma proteins, but is also efficient to avoid reticuloendothelial system phagocytosis and reduce renal excretion, thus, the drug could circulate in the blood for a long time.[11] DOX has also been encapsulated in micelles to achieve passive targeting of the drug, and thereby, reducing adverse effects of the drug.[10] Micelles can be formed by simple self-assembling in solution. Considering that, micelles may be characterized by an easier preparation and a higher scale-up feasibility in comparison to other nanocarriers, such as polymeric nanoparticles and liposomes that require more complex, long-lasting, and costly manufacturing procedures.[12]

In contrast to micelles formed by surfactants of low molecular weight, polymeric micelles are associated with main advantages like lower critical micelle concentration (CMC) and higher kinetic stability.[13] One of the representatives is Genexol PM, which is a polymeric-micelle formulation loading 16 wt% of paclitaxel (PTX) and approved in South Korea.[14] However, due to the complex structure of nanoparticles and potential immunogenicity, novel amphiphilic materials with superior physical and chemical properties have been extensively explored.[15]

Surfactant XR17 has been employed in Apealea,[16] a marketed PTX micelle approved by the European Medicines Agency in 2018. XR17 is a mixture of two *iso*-forms of *N*-

retinoyl-*L*-cysteic acid methyl ester sodium salt, which are both amphiphilic compounds with well-defined structures and low molecular weights. However, XR17 is unstable in the context of light, heat, and oxygen because its structure contains retinol, which is responsible for its rapid degradation.[17] However, acitretin could avoid the reaction of conjugated rearrangement and oxidation of the retinol ring, and thus it has a stable structure.[18] In this study, we tried to replace the retinol part of XR17 with an acitretin to overcome the poor stability of XR17. The new amphiphilic surfactant, namely ACMeNa, was synthesized from acitretin and *L*-cysteic acid methyl ester (LAME) through an amide bond, and then self-assemble in water to form micelles at concentrations above CMC. ACMeNa can not only stably encapsulate lipophilic drugs including docetaxel,[19] but also stably encapsulate water-soluble drugs including DOX. In this work, DOX-loaded polymeric micelles (ACM-DOX) were prepared via a microfluidic method. Our data suggested that ACM-DOX micelles were good in morphology, particle size, and stability, and associated with high entrapment efficiency (EE) and drug loading. ACM-DOX may represent a valuable strategy for the delivery of DOX in clinical treatment.

Materials and Methods

Materials

Acitretin was purchased from Nanjing Dulai Biotechnology Co., Ltd. (Jiangsu, China). All chemicals, of the analytical grade, were obtained from Sinopharm Chemical Reagent Co., Ltd. (Shanghai, China). DOX was procured from Hubei Jiufenglong Chemical Co., Ltd. (Hubei, China).

Cell Culture

A human breast adenocarcinoma cell line (MDA-MB-231) was purchased from Dalian Meilun Biotechnology Co., Ltd. (Dalian, China). MDA-MB-231 cells in Dulbecco's modified Eagle's medium (DMEM) with 10% fetal bovine serum were plated into sterile 96-well plates at 5×10^3 cells/well and incubated in a 5% CO_2 incubator at 37°C.

Synthesis of ACMeNa

An amphiphilic drug carrier of *N*-(9-(4-methoxy-2,3,6-trimethylphenyl)-3,7-dimethyl-2,4,6,8-nonatetraenoyl)-*L*-cysteic acid methyl ester sodium salt (ACMeNa) was synthesized according to a previous report (►**Fig. 1**).[19] Briefly, a mixture of acitretin (3 mmol) and triethylamine (TEA; 10 mmol) in tetrahydrofuran–acetonitrile (ACN) (1:2) was stirred at −20° C, followed by slow addition of butylchloroformate (9.9 mmol). The resulting solution was stirred for 30 minutes, then, LAME (13.5 mmol), *N*,*N*-dimethylformamide (60 mL), and TEA (2.4 mL) were added. The reaction mixture was stirred for 2.5 hours at 25°C. The solvent was evaporated. The residue was washed with saturated aqueous sodium bicarbonate ($NaHCO_3$) and methyl *tert*-butyl ether. After the aqueous solution was saturated with sodium chloride, ethyl acetate was added for extraction and the combined organic layers were dried, filtered, and concentrated sequentially.

Characterization of ACMeNa

ACMeNa was characterized using proton nuclear magnetic resonance (^{1}H NMR; Bruker, ASCEND 400 MHz) and electrospray ionization mass-spectrometry (ESI-MS; Q-TOF micro, Waters, United States) analysis.

High-performance liquid chromatography (HPLC) was used to assess the stability of ACMeNa in solid under different temperatures and light conditions for successive 120 days. Analysis was performed using a reverse-phase HPLC with C18 column (250 mm × 4.6 mm, 5 µm). ACN (containing 20 mmol/L potassium dihydrogen phosphate) in water (55/45, v/v) was used as an eluent. UV detection was performed at 350 nm and the column temperature was 40°C. The flow rate was set at 1.2 mL/min. Each sample was dissolved in methanol (0.5 mg/mL), and 10 µL of which was injected for HPLC analysis.

Preparation of the ACM-DOX Micelles

Micelles were prepared using the microfluidics system with carrier and DOX at a ratio of 1.8:1 (w/w). Then 5.8 mg/mL of DOX was prepared by dissolving a certain amount of DOX in water. An ACMeNa solution (5.1 mg/mL of) was prepared by dissolving ACMeNa in water followed by adjusting the pH to approximately 6 using dilute hydrochloric acid. Both the solutions were prepared independently for separate inlets and mixed within the chip. Herein, an in-plane micromixing structure called Tesla mixer was used. Flow rates of the solutions of DOX and ACMeNa were 3 and 6 mL/min,

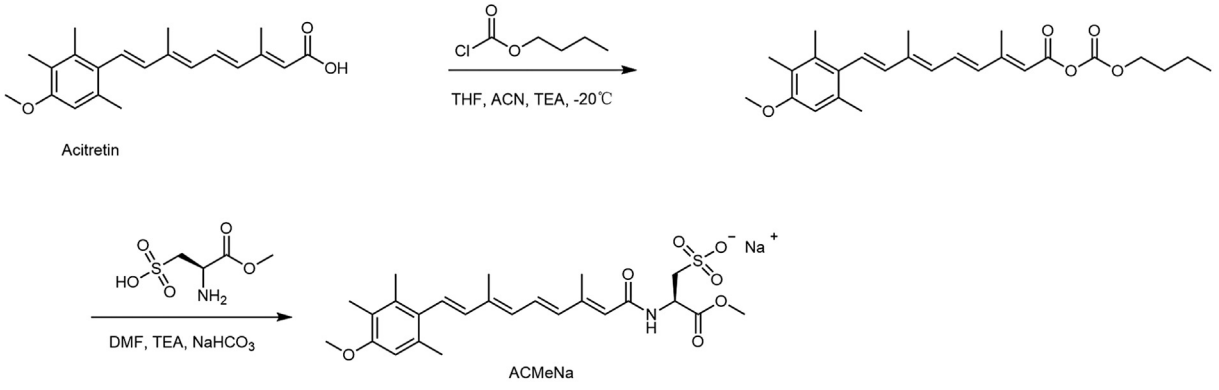

FIg. 1 Synthesis scheme of ACMeNa.

respectively, and controlled with syringe pumps. The micellar solution was filtered through a 0.22 μm microporous membrane filter to obtain micelles, which were lyophilized with a freeze dryer (VirTis Advantage, SP Scientific) through a designed procedure. The obtained micelle formulation was named ACM-DOX.

Study of the Drug-loading Mechanism of ACM-DOX Micelles

Preparation of ACMeNa/DOX Complex and ACMeNa/DOX Physical Mixtures

Our preliminary experiment of preparing DOX-loaded micelles suggested that when DOX solution was added dropwise to the ACMeNa solution, turbidity appears, and after shaking, the precipitate disappeared and the solution became clear. When the ACMeNa solution was added dropwise to the DOX solution, obvious turbidity appeared, but after shaking, the precipitation remained undissolved. It may be speculated that an insoluble ACMeNa/DOX complex was formed.

ACMeNa/DOX complexes were prepared to reveal the assembly mechanism of the ACM-DOX micelle. Briefly, ACMeNa solution (1 mL) was added dropwise into the DOX solution (23.2 mg/mL in water, 4 mL) under magnetic stirring. Stirring was continued for a further 10 minutes after the formation of a suspension. Then, it was centrifuged at 7,500 *g* for 10 minutes. The supernatant was discarded. The precipitate was resuspended in water, vortexed briefly, and centrifuged. The operation was repeated until a clear upper liquid was obtained. The precipitate was filtered and dried under vacuum at 40°C for 24 hours to obtain the ACMeNa/DOX complex.

Physical mixtures of ACMeNa/DOX were prepared by mixing ACMeNa (20.4 mg) and DOX powders (23.2 mg) using a vortex mixer for 1 minute.

Characterization of ACMeNa/DOX Complex

Differential scanning calorimetry (DSC), powder X-ray diffraction (PXRD), and Fourier-transform infrared spectroscopy (FTIR) were used for the characterization of ACMeNa, DOX, ACMeNa/DOX complex, as well as the physical mixtures of ACMeNa/DOX.

The thermal behavior of the samples was analyzed on a DSC (Q2000, TA Instruments) equipped with a refrigerated cooling system. Experiments were performed in a nitrogen atmosphere using approximately 2 mg samples crimpled in aluminum pans. Samples were heated from 40 to 280°C at a heating rate of 10 °C/min.

PXRD data were collected on a Bruker D8 X-ray diffractometer using Cu Kα radiation at 40 kV and 40 mA passing through a nickel filter. Samples were scanned in the 2θ range of 10 to 30°. Measurement was done by placing a powder sample onto a glass plate.

FTIR spectra were measured on a Shimadzu IRTracer-100 spectrometer (Shimadzu, Japan) using KCl pellets. The scanning ranged from 4,000 to 400 cm^{-1} and the resolution was 1 cm^{-1}.

Characterization of ACM-DOX Micelles

Particle Size, Zeta Potential, Morphological, and Stability Analyses

Dynamic light scattering (DLS; Nicomp 380 N3000, PSS Company, United States) was used to assess particle size, polydispersity index, and zeta potential of the ACM-DOX micelles at 25°C. Cryo-transmission electron microscopy (Cryo-TEM; Talos F200C, Thermo Scientific, United States) was used to investigate the morphological features. Particle stability was investigated using the same method after reconstitution over 8 hours with 4- to 32-fold dilutions of their reconstituted solutions.

Determination of Entrapment Efficiency and Drug Loading Efficiency

First, 16 mg of the ACM-DOX micelles was reconstituted in 3 mL water. Unentrapped drug was removed by ultrafiltration centrifugation (7,500 *g*, 20 minutes). HPLC (Shimadzu, Japan) was used to determine the amount of DOX encapsulated. The system was equipped with a C18 column (250 mm × 4.6 mm, 5 μm) with a detection wavelength at 254 nm. The mobile phase consists of 0.01 mol/L sodium lauryl sulfate solution, ACN, and methanol at a ratio of 50:50:6 (v/v). The flow rate was 1 mL/min. The injected sample volume was 10 μL. The calibration curve for DOX was obtained from standard solutions of DOX with the concentration ranging from the analyte limit of quantification (0.001) up to 1.0 mg/mL, with the regression coefficient greater than 0.999. EE and drug loading efficiency (DLE%) were calculated using the following Eqs. (1) and (2):

$$\mathrm{EE} = \frac{\text{Weight of encapsulated DOX in micelles}}{\text{Total weight of DOX}} \times 100\% \quad (1)$$

$$\mathrm{DLE} = \frac{\text{Weight of encapulated DOX in micelles}}{\text{Weight of final formulation}} \times 100\% \quad (2)$$

Determination of the Critical Micelle Concentration

Pyrene was used as a fluorescent probe to estimate CMC, according to a reported study.[20] Briefly, pyrene (1 mg/mL) was dissolved in acetone to achieve a final concentration of 6×10^{-6} mol/L. To a series of vials was added the pyrene solution and evaporated under nitrogen, followed by the addition of different concentrations of ACMeNa aqueous solution (0.00001–1 mg/mL). The mixtures were vortexed for 2 minutes. For each vial, fluorescence intensity was recorded using a spectrofluorometer at an excitation wavelength of 334 nm and emission wavelengths of 375 nm for I_1 and 384 nm for I_3. The CMC was given as the concentration for which an intersection of two straight lines of the I_3/I_1 ratio was observed.

In vitro DOX Release Profile

Drug release of ACM-DOX micelles *in vitro* was evaluated by a dialysis method. An ACM-DOX micelle solution containing 1.93 mg of DOX was added to a dialysis bag (8,000–140,000 Da). Then the dialysis bag was placed into a container with

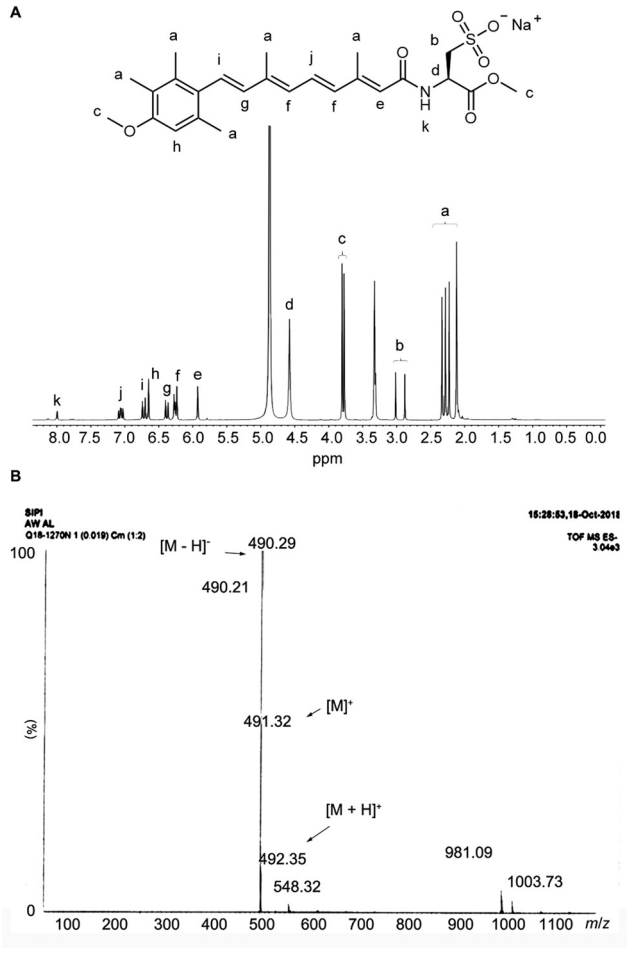

FIg. 2 (A) ^{1}H NMR and **(B)** ESI-MS spectra of ACMeNa.

40 mL of acetate buffer (pH = 5.0) supplemented with 20% v/v ethanol at 37 ± 0.5°C/100 rpm. Samples of the release solution (1 mL) were removed at different time points and immediately replaced by 1 mL of the release medium ($n = 3$). A parallel dialysis, in which a dialysis bag containing the same amount of free DOX, was conducted for comparison. The concentration of DOX in the dissolution medium was determined using HPLC as described in the section "Determination of Entrapment Efficiency and Drug Loading Efficiency."

Cytotoxicity Assay

Cell Counting Kit-8 (CCK-8) was used to assess cell viability. Briefly, aliquots (100 µL) of MDA-MB-231 cells were seeded in a 96-well plate (5×10^3 cells/well) and incubated for 24 hours before the experiment. MDA-MB-231 cells were treated with 100 µL of DMEM containing different concentrations of DOX, ACMeNa, and ACM-DOX micelles, and incubated for 24 hours. The micelle concentration was calculated depending on the DOX content. At the same time, cells treated with DMEM were used as a blank control. The culture medium was removed. Cells were washed twice with PBS, mixed with 100 µL of culture medium containing 10% CCK-8, and incubated for another 2 hours. Cell viability (%) was calculated based on absorbance at 450 nm, measured by a microplate reader (Thermo Scientific Multiskan FC). Each group has six wells.

Results and Discussion

Successful Synthesis of ACMeNa

ACMeNa was first synthesized from acitretin, based on a method mentioned in the section "Synthesis of ACMeNa," with a yield of 82% and purity of 99.69%. As shown in ►**Fig. 2A**, ^{1}H NMR (400 MHz, CD_3OD) δ 8.00 (s, 1H), 7.05 (dt, $J = 23.1$, 11.5 Hz, 1H), 6.72 (d, $J = 16.3$ Hz, 1H), 6.65 (s, 1H), 6.38 (d, $J = 15.0$ Hz, 1H), 6.30–6.20 (m, 2H), 5.93 (s, 1H), 4.58 (s, 1H), 3.80 (s, 3H), 3.77 (s, 3H), 3.02 (s, 1H), 2.88 (s, 1H), 2.38–2.03 (m, 15H). ESI-MS revealed m/z $[M - H]^-$ 490.21, m/z $[M]^+$ 491.32, and m/z $[M + H]^+$ 492.35 (►**Fig. 2B**), corresponding to the ACMeNa molecular weight. Based on these results, we conclude that ACMeNa was successfully synthesized.

The chemical stability of solid ACMeNa is shown in ►**Table 1**. Our data showed that ACMeNa had a good stability when protected from light at −18°C and 4°C. However, at 120 days, approximately 2% ACMeNa was degraded at ambient temperature (25°C), in the presence of light or protected from light. Our data recommended ambient storage of ACMeNa in the dark.

Table 1 Chemical stability of ACMeNa in solid

Time (d)	Normal ambient light assay at 25°C (%)	Protected from light assay at 25°C (%)	Protected from light assay at 4°C (%)	Protected from light assay at −18°C (%)
0	99.87	99.87	99.87	99.87
1	99.24	99.34	99.57	99.70
3	99.11	99.13	99.30	99.69
7	99.09	99.12	99.25	99.61
30	98.99	98.97	99.26	99.54
60	98.91	98.93	99.16	99.51
90	98.85	98.55	99.05	99.45
120	98.84	98.19	99.04	99.21

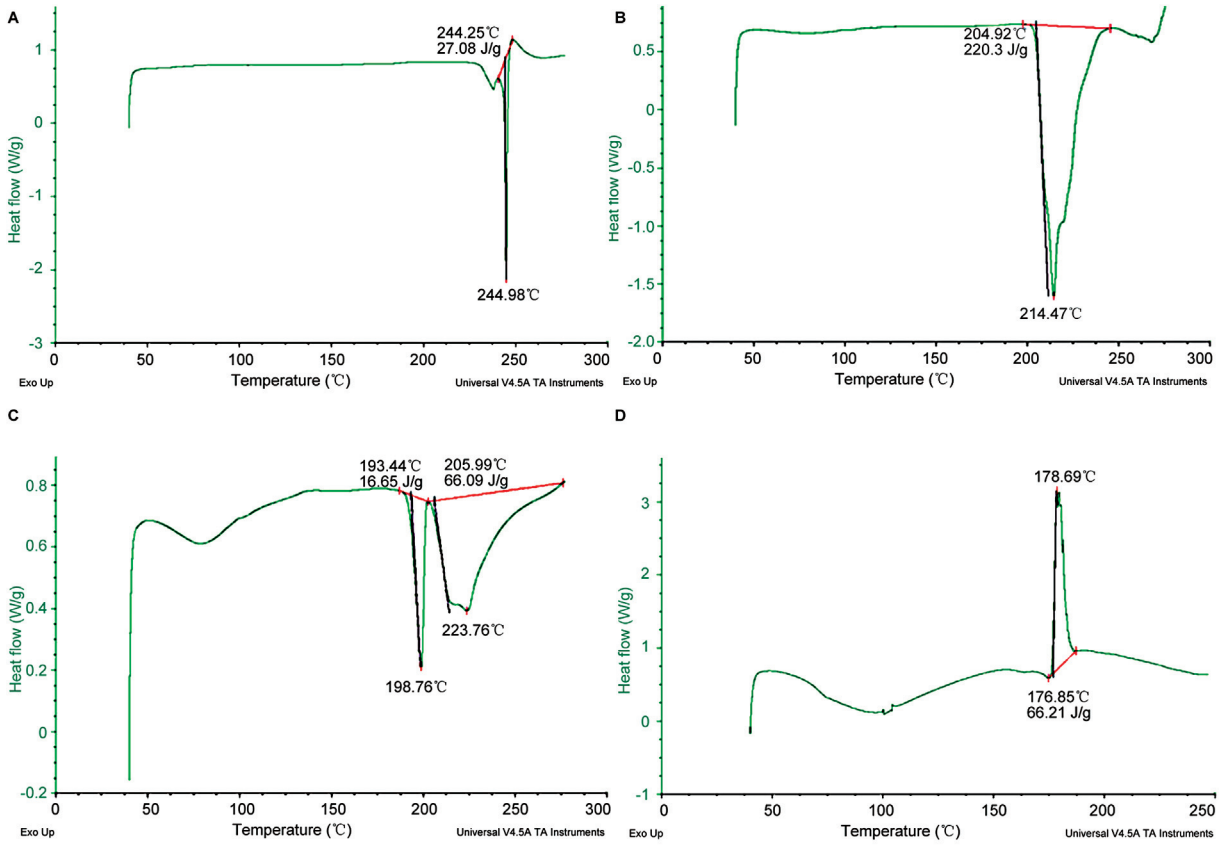

FIg. 3 DSC spectra of **(A)** ACMeNa, **(B)** DOX, **(C)** ACMeNa/DOX physical mixtures, and **(D)** ACMeNa/DOX complex.

Formation Mechanism of ACM-DOX Micelles

DSC is a powerful tool to reflect the purity, crystalline form, and stability of substances by measuring the thermal effects of substances in the process of phase transition so as to distinguish and identify different substances.[21] As shown in ►**Fig. 3**, there is a single endothermic peak in DSC plots of both ACMeNa and DOX, indicating a high purity of the two substances. However, in comparison to ACMeNa or DOX, there are two endothermic peaks of physical mixtures of ACMeNa/DOX that shifted to the left, and this was consistent

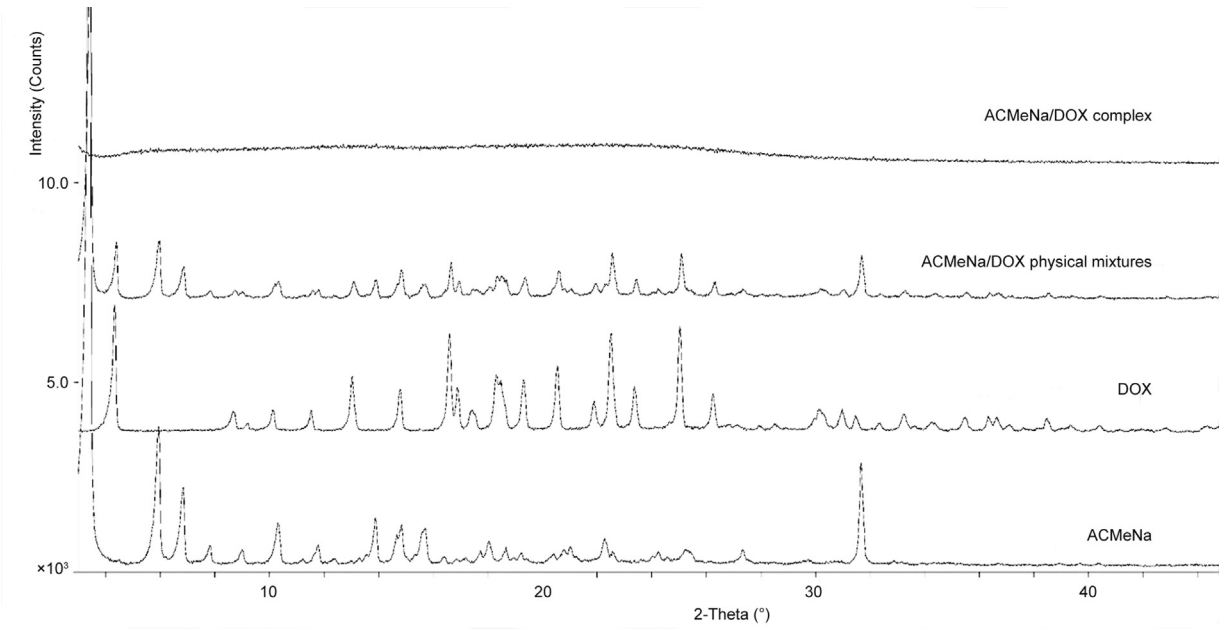

FIg. 4 PXRD spectra of ACMeNa, DOX, ACMeNa/DOX physical mixtures, and ACMeNa/DOX complex.

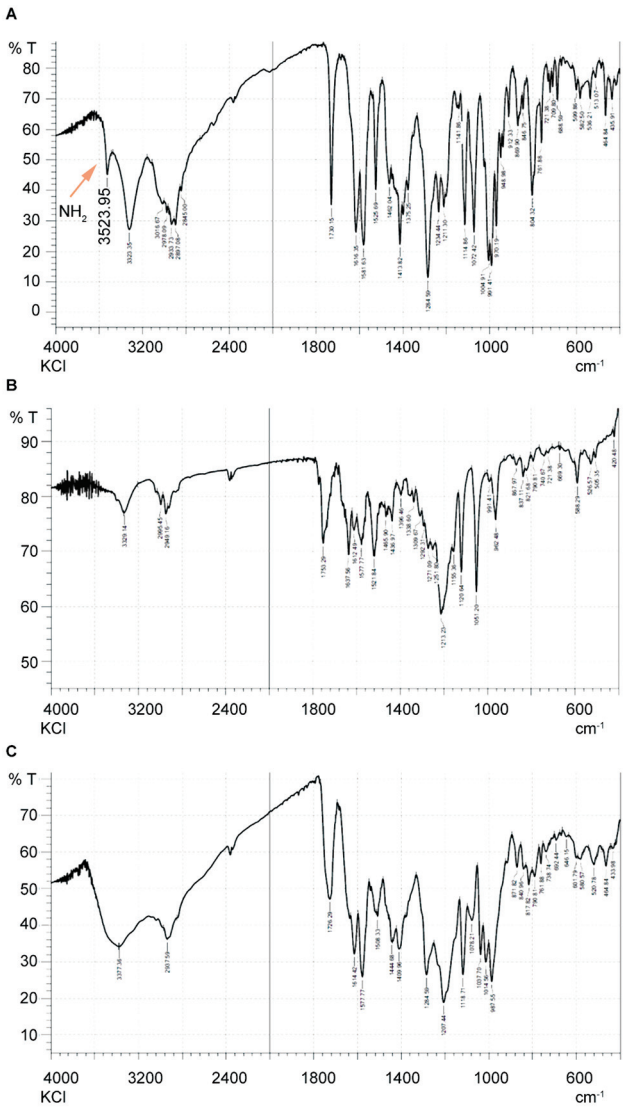

FIg. 5 FTIR spectra of **(A)** ACMeNa, **(B)** DOX, and **(C)** ACMeNa/DOX complex.

with the melting-point depression rule for mixtures. Interestingly, only one exothermic peak was found in the ACMeNa/DOX complex, which was distinct from the other three samples, indicating that the ACMeNa/DOX complex existed in a unique form.

PXRD can qualitatively and quantitatively analyze the crystalline morphology of solid substances and reflect small changes in the crystalline composition of solid drug components in the PXRD patterns.[22] ►**Fig. 4** demonstrates a crystalline state of ACMeNa and DOX. The peaks of PXRD patterns of ACMeNa/DOX physical mixtures are nearly a superposition of spectra of ACMeNa and DOX. However, almost no diffraction peak of the ACMeNa/DOX complex is observed, implying an amorphous state of the complex. Combined with the results of DSC patterns (►**Fig. 3**), the ACMeNa/DOX complex was in an amorphous state, and the exothermic peak in the DSC may be generated when the complex transformed from an amorphous state to a crystalline state.

Through detecting the subtle changes in functional groups of the chemical structure in FTIR spectroscopy,[23] interaction between the sulfonic acid group of ACMeNa and the amino group of DOX was assessed. In ►**Fig. 5**, the infrared spectrum of the ACMeNa/DOX complex was a superposition of ACMeNa and DOX spectra, and the characteristic absorption peaks corresponding to ACMeNa and DOX were shown in the infrared spectrum of the ACMeNa/DOX complex, indicating no new chemical bond is formed between ACMeNa and DOX. However, subtle changes in characteristic peaks in the fingerprint region of the ACMeNa/DOX complex demonstrated hydrogen bonds or van der Waals forces between ACMeNa and DOX. At the same time, the amino stretching vibration peak disappeared at 3,500 cm^{-1}, indicating that the amino group contributed to the formation of the ACMeNa/DOX complex.

Above all, an amorphous form of the ACMeNa/DOX complex may be a result of electrostatic interaction between the sulfonic acid group of ACMeNa carriers and the amino group of DOX. Therefore, the ACMeNa/DOX complex may be involved in the process of DOX loading. It can be speculated that an insoluble ACMeNa/DOX complex (7 μg/mL in water; DOX concentration of the supernatant in the section "Preparation of ACMeNa/DOX Complex and ACMeNa/DOX Physical Mixtures" was determined using HPLC as described in the section "Determination of Entrapment Efficiency and Drug Loading Efficiency") was first formed, and subsequently encapsulated by the excessive carriers during the self-assembly process to form ACM-DOX micelles.

Characterization of ACM-DOX Micelles

Drugs can be encapsulated in the micelles during their formation, or in a second step, depending on the method used for preparation. Micelles can be prepared by different methods including direct dissolution, dialysis, emulsion with solvent evaporation, and solution casting followed by film hydration.[24] When an insoluble drug was encapsulated, environmentally unfriendly organic solvents were inevitably used in those methods. Encouragingly, DOX and ACMeNa are soluble in water, and the limitation of the organic solvents can be avoided. Considering easy manipulation conditions and high scale-up feasibility, microfluidic devices were used to prepare DOX-loaded ACM-DOX micelles (►**Fig. 6A**). The microchannel schematic is shown in ►**Fig. 6B**: DOX solution was mixed with the carrier at a volume ratio of 1:2. At the junction of the streams, enhanced mixing occurs through the Tesla structures as the focused streams flow along the channel. Given that properties such as polarity and hydration degree of micelles are not uniform within the carrier, drugs can be hosted in different sites, close to the surface or in the inner core, depending on their properties. Most of the time, hydrophobic drugs are loaded and hosted in the inner core. Due to the lipophilic nature of the ACMeNa/DOX complex, DOX could be incorporated into the micelle core at a carrier/drug ratio of 1.8:1 (w/w). Thus, in the present study, the ACM-DOX micelles were prepared using a microfluidic method that does not require organic solvents.

The smaller size of the micelles is suitable for passive tumor targeting,[25] and the smaller negative zeta potential of the surface was associated with a lower protein adsorption, which

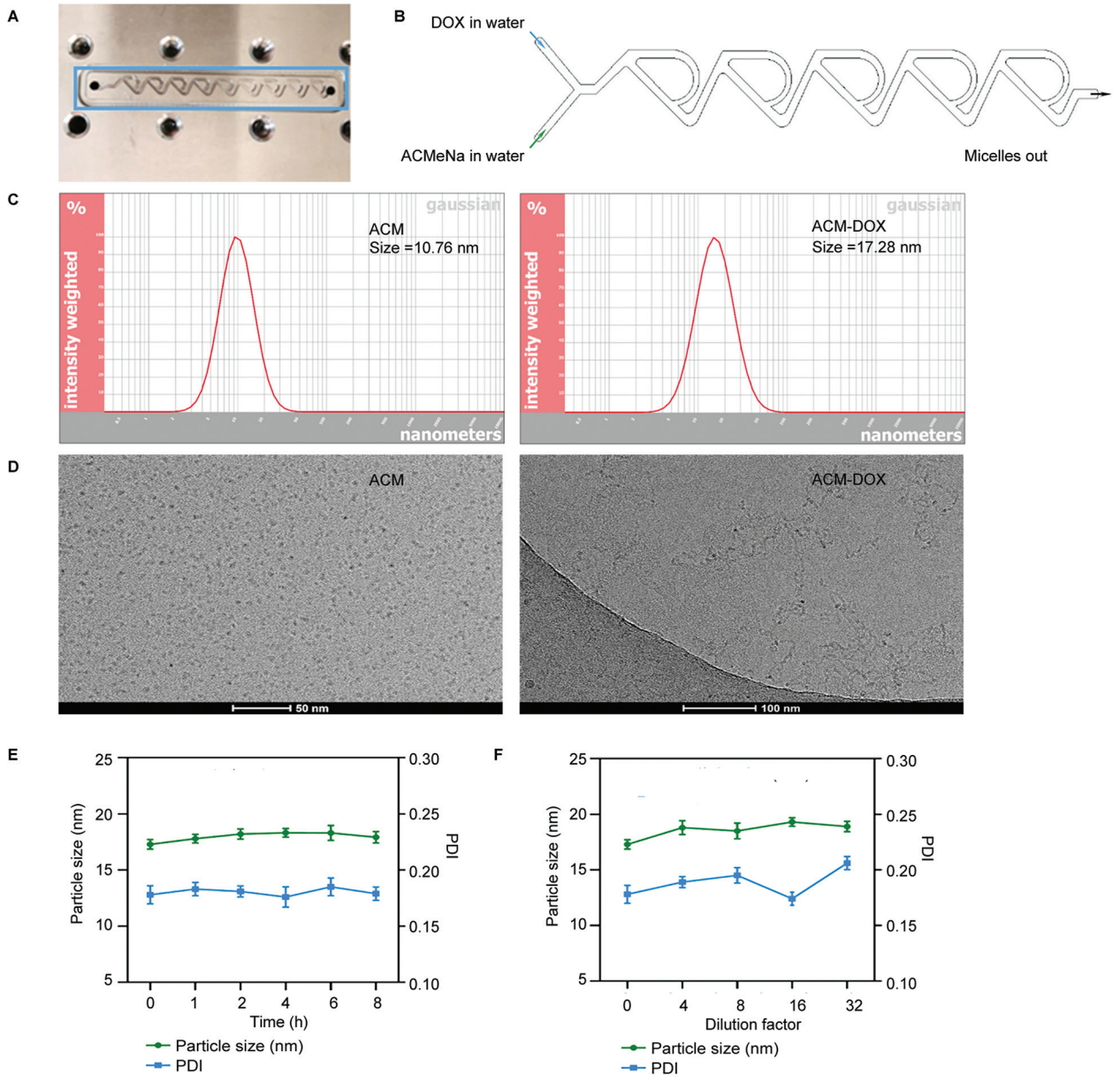

FIg. 6 (A) Micro-fluidic device with Tesla mixer. **(B)** A representative schematic of input and output streams within ACM-DOX micelle formation in micro-channels with Tesla structures. **(C)** DLS analysis of size distribution of micelles of blank ACM and ACM-DOX. **(D)** Cryo-TEM image of micelles of blank ACM and ACM-DOX. **(E)** Stability of ACM-DOX micelles after reconstituted assayed by the size and polydispersity index over 8 hours. **(F)** Stability of ACM-DOX micelles following dilution with water at different folds assayed by the size and polydispersity index. All results are displayed as mean ± standard deviation ($n = 3$). DLS, dynamic light scattering; TEM, transmission electron microscopy.

avoids mononuclear phagocyte system clearance and prolongs the circulation lifetime of the drug.[26,27] Consistent with this, in this work, low particle size (19.4 ± 0.2 nm) (►**Fig. 6C**) and zeta potential (−43.7 ± 2.4 mV) were also detected for our ACM-DOX micelles. At mean time, ACM-DOX micelles also exhibited high EE (92.4 ± 0.5%) and DLE (33.4 ± 0.3%). DLS results showed a size of 10.76 and 17.28 nm of blank ACM and ACM-DOX micelles, respectively, suggesting the comparable size of the two micelles (►**Fig. 6C**). Cryo-TEM results showed a spherical system of blank ACM micelles, and a worm-like morphology of ACM-DOX micelles (►**Fig. 6D**), which was also found in squalenoylated doxorubicin micelles reported by Maksimenko et al.[28] A micellar shape can be influenced by different factors including the structure of carriers used, as well as the surrounding environment in terms of temperature, pH, and composition. As for squalene-acylated doxorubicin micelles, the concentration of loading drugs, ionic strength, and anionic properties have been reported to affect the morphology of micelles.[29] However, these factors may not affect the worm-like appearance of ACM-DOX micelles, but may be closely associated with the unique interaction between carriers and DOX. This can be supported by a previous reported study,[30] in which cetyltrimethyl-ammonium bromide (CTAB) formed worm-like CTAB/NaSal micelles at lower concentrations, in the presence of sodium salicylate (NaSal).

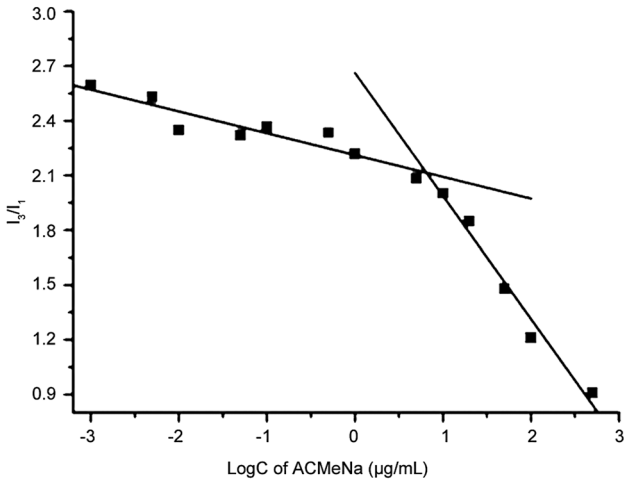

FIg. 7 CMC determination of ACMeNa. CMC, critical micelle concentration.

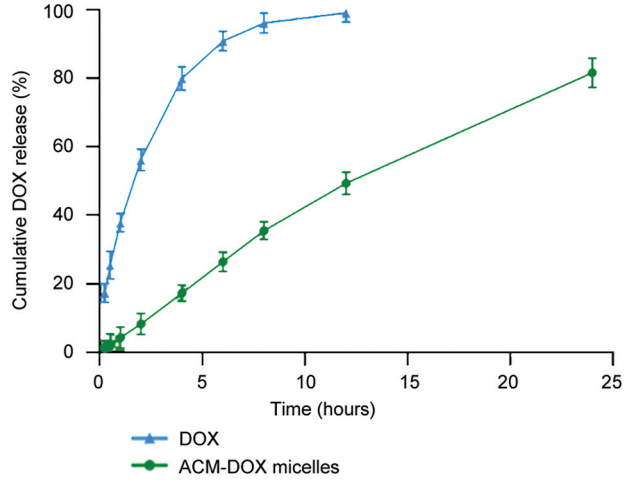

FIg. 8 Drug release profiles of free DOX and ACM-DOX micelles. Data are expressed as mean ± standard deviation ($n = 3$).

Micelle morphology was fundamental in predicting micelles' behavior *in vivo*, as the shape of nanocarriers plays a key role in influencing the circulation time, biodistribution, and cellular uptake. For instance, the soft and flexible nature of worm-like micelles could minimize phagocytosis,[31] prolong their circulation in the blood,[32] and increase maximum tolerated dose.[33] Thus, worm-like ACM-DOX micelles were more likely to be favored in delivering and releasing DOX at tumor sites. Notably, in this study, a stable average particle size of approximately 20 nm was obtained within 8 hours after the reconstitution of the lyophilized powders with water (►**Fig. 6E**). The particle size and size distribution did not change upon 32-fold dilution of the initial dispersion (►**Fig. 6F**), indicating their superior colloidal stability.

The pyrene method was used for CMC determination, due to its high sensitivity and easy application.[34] The CMC of ACMeNa was determined by plotting fluorescence intensity (using pyrene as a fluorescent probe) against ACMeNa concentration. Our data confirmed a low CMC of ACMeNa, approximately 6.50 μg/mL (►**Fig. 7**), which is much lower than those of conventional surfactants, such as sodium dodecyl sulfate (2.39 mg/mL) and reported polypeptide, and similar to those of PEG-poly(amino acid) block copolymers used in clinical trials.[35,36] Due to low CMC, ACM-DTX micelles could remain stable at very low ACMeNa concentrations, which makes them relatively insensitive to dilution (as described above with 32-fold dilution), resulting in an enhanced circulation time of the drug.

Furthermore, a release study was performed at pH 5.0 to mimic a low pH value of tumor environments.[37] Our data suggested that free DOX diffused out of the dialysis bag was 80.0 ± 0.5% in the first 4 hours, and 99.1 ± 2.3% at 12 hours (►**Fig. 8**), suggesting a rapid release profile of free DOX. However, the released DOX from ACM-DOX micelles was only 17.3 ± 0.4% in first 4 hours, 49.4 ± 1.3% at 12 hours, and 81.7 ± 4.3% at 24 hours, suggesting a slower release profile of DOX from ACM-DOX micelles in comparison to free DOX. Then, various mathematical models were applied to evaluate *in vitro* drug release profile of ACM-DOX micelles, including zero-order kinetics, first-order kinetics, the Higuchi model, the Hixson–Crowell model, and the Ritger–Peppas formula model (►**Table 2**). Correlation coefficient (R^2) analysis showed that ACM-DOX micelles have a sustained release effect to some extent, and first-order kinetics, with $R^2 = 0.9991$, turned out to be the most suitable model to describe the release profile of DOX from ACM-DOX micelles.

ACM-DOX Micelles Inhibited Viability of MDA-MB-231 Cells

As shown in ►**Fig. 9A**, the carrier ACMeNa exhibited almost no cytotoxicity, and the cells maintained a survival rate of 86.20 ± 4.66% even at a high concentration (100 μg/mL), indicating a good cell compatibility of the carrier. DOX and ACM-DOX micelles inhibited cell viability of MDA-MB-231

Table 2 Drug cumulative release kinetics results of ACM-DOX micelles

Model	Equation	*a*	*b*	R^2
Zero-order	$Y = a\,X + b$	3.470	2.908	0.9813
First-order	$Y = b\,(1 - e^{-ax})$	0.032	151.811	0.9991
Higuchi	$Y = a\,X^{1/2} + b$	18.431	−14.272	0.9702
Hixson–Crowell	$(100 - Y)^{1/3} = -a\,X + b$	0.078	4.653	0.9947
Weibull	$In[In(100/(100 - Y))] = a\,InX + b$	1.207	−3.342	0.9990
Ritger–Peppas	$Y = a\,X^b$	5.977	0.828	0.9949

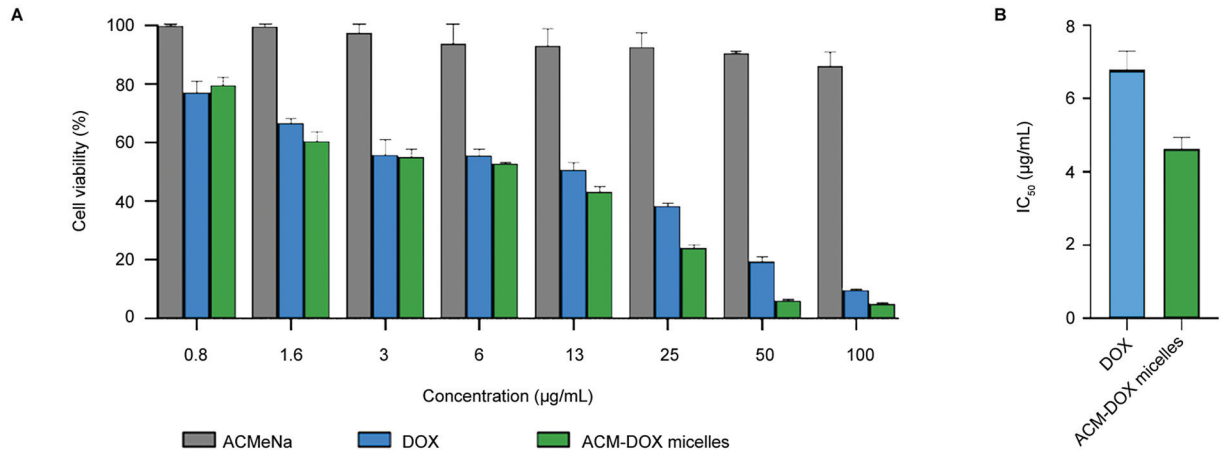

FIg. 9 (A) *In vitro* cytotoxicity of MDA-MB-231 after treatment with different concentrations of DOX, ACMeNa, and ACM-DOX micelles. **(B)** IC_{50} values of MDA-MB-231 treated with DOX and ACM-DOX micelles.

cells in a dose-depended manner. At the same concentration, the cytotoxicity of ACM-DOX micelles was significantly higher than that of free DOX. Besides, IC_{50} values of DOX and ACM-DOX were 6.80 ± 0.50 and 4.64 ± 0.32 μg/mL, respectively (►**Fig. 9B**). Given above, ACMeNa is noncytotoxic, and in comparison to free DOX, DOX encapsulated in ACM-DOX micelles was more cytotoxic.

Conclusion

In this work, a novel and stable amphiphilic surfactant, ACMeNa, was synthesized to encapsulate water-soluble DOX to control the release and enhance the efficiently of the drug. ACM-DOX micelles can be prepared by a microfluidic method, which avoided the use of organic solvents, and was highly feasible to scale up. The mechanism of micelle formation suggested that an insoluble ACMeNa/DOX complex was formed by electrostatic interaction, and then effectively encapsulated to form ACM-DOX micelles during self-assembly. ACM-DOX micelles had a worm-like morphology, a particle size distribution of approximately 20 to 100 nm, as well as high EE% and DLE%. Moreover, ACM-DOX micelles were associated with good dilution stability *in vitro* and a slow-release effect, and showed significant concentration-dependent toxicity. The strategy of ACMeNa as nanocarriers provides a means to encapsulate water-soluble DOX. The stability and size of worm-liked ACM-DOX micelles make them particularly suitable for cancer therapy with tumor-selectivity potential. Further work will focus on analyzing the exact localization ACM-DOX micelles and their efficacy *in vivo*.

Conflicts of Interest

The authors declared that there are no conflicts of interest.

References

1 Tacar O, Sriamornsak P, Dass CR. Doxorubicin: an update on anticancer molecular action, toxicity and novel drug delivery systems. J Pharm Pharmacol 2013;65(02):157–170
2 Prathumsap N, Shinlapawittayatorn K, Chattipakorn SC, Chattipakorn N. Effects of doxorubicin on the heart: From molecular mechanisms to intervention strategies. Eur J Pharmacol 2020; 866:172818
3 Takemura G, Fujiwara H. Doxorubicin-induced cardiomyopathy from the cardiotoxic mechanisms to management. Prog Cardiovasc Dis 2007;49(05):330–352
4 Carvalho C, Santos RX, Cardoso S, et al. Doxorubicin: the good, the bad and the ugly effect. Curr Med Chem 2009;16(25):3267–3285
5 Cagel M, Grotz E, Bernabeu E, Moretton MA, Chiappetta DA. Doxorubicin: nanotechnological overviews from bench to bedside. Drug Discov Today 2017;22(02):270–281
6 Haley B, Frenkel E. Nanoparticles for drug delivery in cancer treatment. Urol Oncol 2008;26(01):57–64
7 Xing M, Yan F, Yu S, Shen P. Efficacy and cardiotoxicity of liposomal doxorubicin-based chemotherapy in advanced breast cancer: a meta-analysis of ten randomized controlled trials. PLoS One 2015;10(07):e0133569
8 Rafiyath SM, Rasul M, Lee B, Wei G, Lamba G, Liu D. Comparison of safety and toxicity of liposomal doxorubicin vs. conventional anthracyclines: a meta-analysis. Exp Hematol Oncol 2012;1 (01):10
9 Chen E, Chen BM, Su YC, et al. Premature drug release from polyethylene glycol (PEG)-coated liposomal doxorubicin *via* formation of the membrane attack complex. ACS Nano 2020;14(07): 7808–7822
10 Zhang Y, Huang Y, Li S. Polymeric micelles: nanocarriers for cancer-targeted drug delivery. AAPS PharmSciTech 2014;15 (04):862–871
11 Lu Y, Zhang E, Yang J, Cao Z. Strategies to improve micelle stability for drug delivery. Nano Res 2018;11(10):4985–4998
12 Paliwal R, Babu RJ, Palakurthi S. Nanomedicine scale-up technologies: feasibilities and challenges. AAPS PharmSciTech 2014;15 (06):1527–1534
13 Adams ML, Lavasanifar A, Kwon GS. Amphiphilic block copolymers for drug delivery. J Pharm Sci 2003;92(07):1343–1355
14 Stirland DL, Nichols JW, Miura S, Bae YH. Mind the gap: a survey of how cancer drug carriers are susceptible to the gap between research and practice. J Control Release 2013;172(03):1045–1064
15 Hwang D, Ramsey JD, Kabanov AV. Polymeric micelles for the delivery of poorly soluble drugs: From nanoformulation to clinical approval. Adv Drug Deliv Rev 2020;156:80–118
16 European Medicines Agency. Assessment report for Apealea. Accessed October 13, 2022 at: https://www.ema.europa.eu/en/documents/assessment-report/apealea-epar-public-assessment-report_en.pdf.

17 Oleg S, Julian A. Retinol derivatives, their use in the treatment of cancer and for potentiating the efficacy of other cytotoxic agents. CN Patent 02829608.7. September, 2005
18 Fu PP, Cheng SH, Coop L, et al. Photoreaction, phototoxicity, and photocarcinogenicity of retinoids. J Environ Sci Health Part C Environ Carcinog Ecotoxicol Rev 2003;21(02):165–197
19 He J, Wang ZF, Zhao YZ, et al. Phenyl-containing compound and intermediate, preparation method and application thereof. CN Patent 112321465A. February, 2021
20 Aguiar J, Carpena P, Molina-Bolívar JA, Carnero Ruiz C. On the determination of the critical micelle concentration by the pyrene 1:3 ratio method. J Colloid Interface Sci 2003;258:116–122
21 Faroongsarng D. Theoretical aspects of differential scanning calorimetry as a tool for the studies of equilibrium thermodynamics in pharmaceutical solid phase transitions. AAPS PharmSciTech 2016;17(03):572–577
22 Onoda H, Inoue Y, Ezawa T, et al. Preparation and characterization of triamterene complex with ascorbic acid derivatives. Drug Dev Ind Pharm 2020;46(12):2032–2040
23 Yao J, Shi NQ, Wang XL. The development of co-amorphous drug systems [in Chinese]. Yao Xue Xue Bao 2013;48(05):648–654
24 Ghezzi M, Pescina S, Padula C, et al. Polymeric micelles in drug delivery: an insight of the techniques for their characterization and assessment in biorelevant conditions. J Control Release 2021; 332:312–336
25 Torchilin V. Tumor delivery of macromolecular drugs based on the EPR effect. Adv Drug Deliv Rev 2011;63(03):131–135
26 Patil S, Sandberg A, Heckert E, Self W, Seal S. Protein adsorption and cellular uptake of cerium oxide nanoparticles as a function of zeta potential. Biomaterials 2007;28(31):4600–4607
27 Alexis F, Pridgen E, Molnar LK, Farokhzad OC. Factors affecting the clearance and biodistribution of polymeric nanoparticles. Mol Pharm 2008;5(04):505–515
28 Maksimenko A, Dosio F, Mougin J, et al. A unique squalenoylated and nonpegylated doxorubicin nanomedicine with systemic long-circulating properties and anticancer activity. Proc Natl Acad Sci U S A 2014;111(02):E217–E226
29 Mougin J, Yesylevskyy SO, Bourgaux C, et al. Stacking as a key property for creating nanoparticles with tunable shape: the case of squalenoyl-doxorubicin. ACS Nano 2019;13(11):12870–12879
30 Lam CN, Do C, Wang Y, Huang GR, Chen WR. Structural properties of the evolution of CTAB/NaSal micelles investigated by SANS and rheometry. Phys Chem Chem Phys 2019;21(33):18346–18351
31 Champion JA, Mitragotri S. Shape induced inhibition of phagocytosis of polymer particles. Pharm Res 2009;26(01):244–249
32 Geng Y, Dalhaimer P, Cai S, et al. Shape effects of filaments versus spherical particles in flow and drug delivery. Nat Nanotechnol 2007;2(04):249–255
33 Christian DA, Cai S, Garbuzenko OB, et al. Flexible filaments for in vivo imaging and delivery: persistent circulation of filomicelles opens the dosage window for sustained tumor shrinkage. Mol Pharm 2009;6(05):1343–1352
34 Sezgin Z, Yüksel N, Baykara T. Preparation and characterization of polymeric micelles for solubilization of poorly soluble anticancer drugs. Eur J Pharm Biopharm 2006;64(03):261–268
35 Yamamoto T, Yokoyama M, Opanasopit P, Hayama A, Kawano K, Maitani Y. What are determining factors for stable drug incorporation into polymeric micelle carriers? Consideration on physical and chemical characters of the micelle inner core. J Control Release 2007;123(01):11–18
36 Oerlemans C, Bult W, Bos M, Storm G, Nijsen JF, Hennink WE. Polymeric micelles in anticancer therapy: targeting, imaging and triggered release. Pharm Res 2010;27(12):2569–2589
37 You JO, Auguste DT. Feedback-regulated paclitaxel delivery based on poly(N,N-dimethylaminoethyl methacrylate-co-2-hydroxyethyl methacrylate) nanoparticles. Biomaterials 2008;29(12):1950–1957